nature geoscience

Brief Communication https://doi.org/10.1038/s41561-022-01096-w

Recovery from microplastic-induced marine deoxygenation may take centuries

In the format provided by the authors and unedited

Supplemental Information

Active trapping of oxygen anomalies in the Southern Ocean

The Southern Ocean has been previously recognized for its potential to trap regenerated silicic acid [1, 2] and alkalinity [3], due to efficient biological uptake which strip both from the euphotic zone, thereby preventing northward lateral transport via shallower water masses. Our results demonstrate a long-term, active trapping of microplastic-induced oxygenation perturbation in the Southern Ocean, as indicated by the persistent oxygen deficit held within the Antarctic Bottom Water and Circumpolar Deep Water masses, in seawater younger than when the microplastic was removed (where seawater age is set to zero in the surface layer, including under sea ice), and in the persistent oxygen surplus held within grid cells under sea ice (Fig. S1, S2).

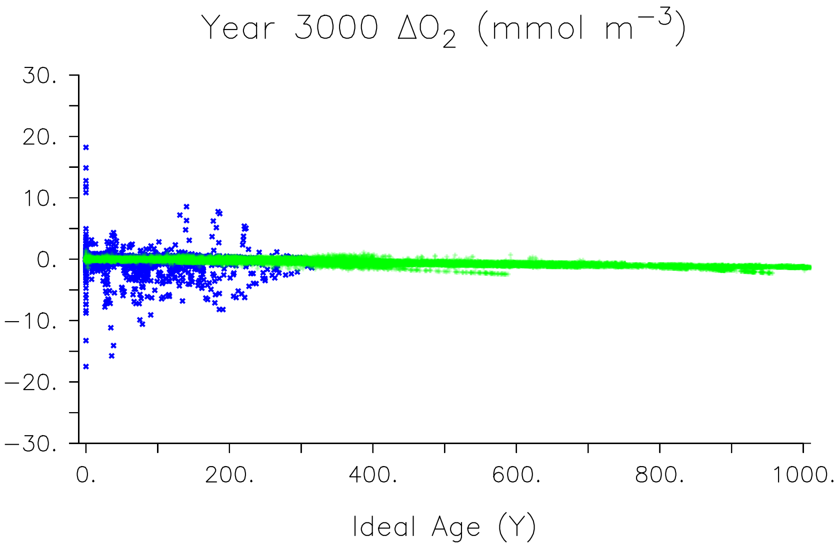

Fig. S1 Year 3000 Southern Ocean MP_{STOP}-CNTL O_2 anomalies in mmol O_2 m^{-3} plotted by water mass age (time since the water parcel last had contact with the ocean surface)[4]. Blue points are grid cells between 90-60°S, green points are grid cells between 60-30°S.

Sustained and propagating oxygen anomalies in the Southern Ocean sea ice regions result from historic microplastic-induced nutrient trapping. Additional nutrients become trapped in the Weddell Sea, under ice (see years 2490-2590 in Fig. S2). These nutrients stimulate additional phytoplankton growth in the Sea, which stimulates additional oxygen consumption in sinking water masses (see corresponding net primary production; NPP, apparent oxygen utilisation; AOU=$O_2 sat$-O_2, and oxygen anomaly plots), which carry the oxygen deficit into the deep ocean. However, sea ice cover traps biogenic oxygen under the ice in the subsurface, (see AOU anomaly plots in the Weddell at year 2590, where a lower AOU anomaly in MP_{STOP} represents additional biogenic oxygen, not reduced utilization, relative to CNTL). This positive oxygen anomaly exits the basin to the west, along the Antarctic coastline and following a different trajectory than the negative oxygen anomaly water masses. A low oxygen anomaly forms in the Ross Sea at year 2690 due to an upwelling event, where additional Southern Ocean-trapped nutrients enhance primary production and consequent loss of water column oxygen. This event also produces a positive oxygen surface anomaly (not shown), which propagates under the ice deeper into the Ross Sea. The divergent trajectories of surface and deep water masses in the Southern Ocean under sea ice cover are responsible for the persistent oxygen anomalies (both positive and negative) we see in our model results.

This microplastic-induced nutrient trapping legacy does not occur in, and therefore does not affect, the deep Arctic, but an additional deoxygenation of the deep North Atlantic of about 0.5 mmol O_2 m^{-3} by the year 3000 when sea ice does not prevent biogenic oxygen loss is recorded in southern-sourced bottom water.

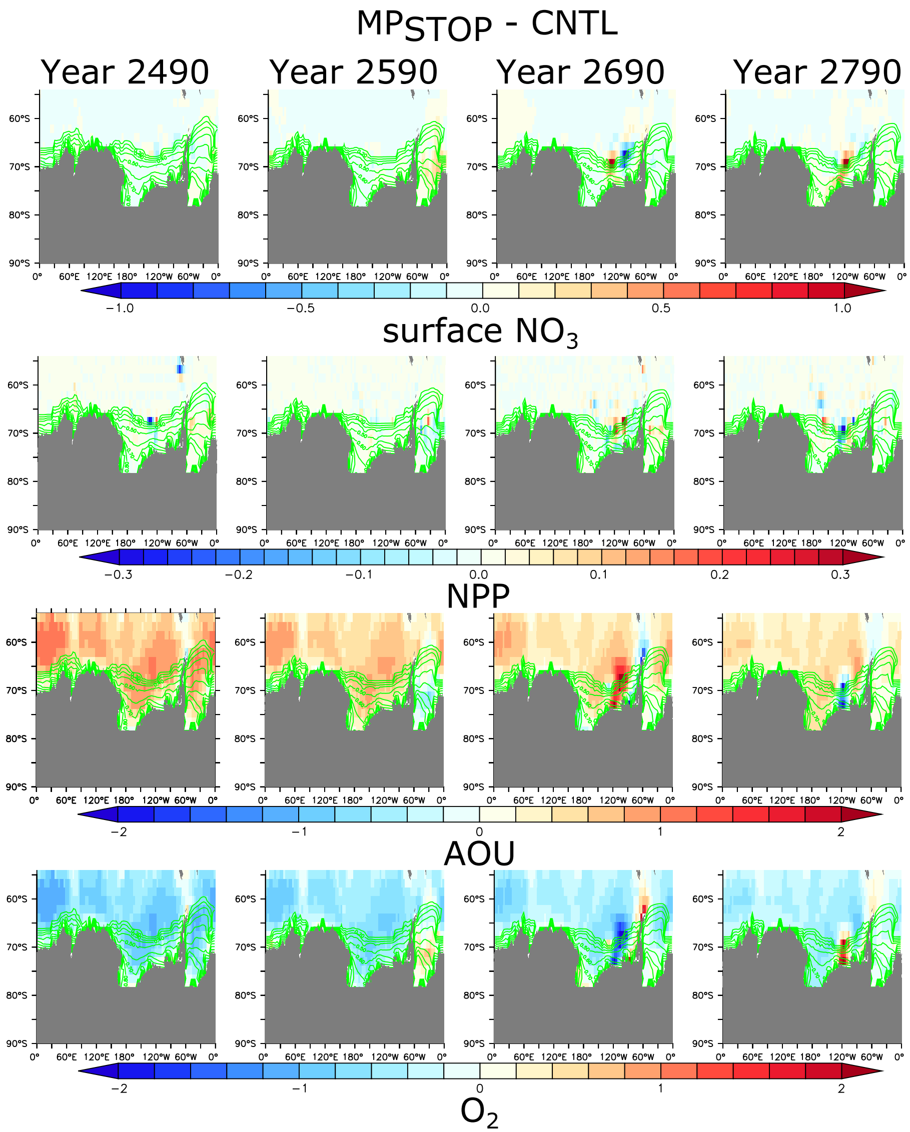

Fig. S2 MP_{STOP}-CNTL anomalies of (top to bottom) surface nitrate in mmol m^{-3}, net primary production in mol N per year, water column average apparent oxygen utilisation (AOU=O_2sat-O_2 in mmol m^{-3}), and average water column oxygen in mmol m^{-3}. Green contours are annual average sea ice fraction.

Mitigation of Southern Ocean oxygen deficits

The influence of sea ice in the mitigation of oxygen deficits becomes apparent when comparing the responses of MP_{STOP}-CNTL and MP_{NOICE}-$CNTL_{NOICE}$

(Fig. S3). Nutrient trapping effects on net primary production are identical, which rules out the possibility for a northern hemisphere-origin of the additional deoxygenation in the NOICE simulations. AOU (O_2sat-O_2) is strongly enhanced when sea ice is removed as an oxygen barrier. Because biological utilisation is the same between MP_{STOP} and MP_{NOICE} models, and the incoming atmospheric flux of O_2 is the same between MP_{NOICE} and $CNTL_{NOICE}$ models, this enhancement must be due to the additional loss of biogenic O_2 under sea ice.

A second set of simulations in which microplastic forcing is not included and in which sensitivity to oxygen exchange through sea ice is permitted is next examined. $CNTL_{NOICE}$ permits two-way oxygen exchange through sea ice. $CNTL_{LOSS}$ permits only ocean oxygen loss through sea ice. $CNTL_{GAIN}$ permits only oxygen gain through sea ice. When oxygen exchange through the sea ice barrier is permitted, biogenic O_2 is allowed to escape to the atmosphere while atmospheric O_2 enters the ocean. The loss of biogenic O_2 in the NOICE simulations reduces the total increase relative to when ice blocks exchange, despite overall higher O_2 concentrations. Biogenic oxygen anomalies are strongest directly under the sea ice, but anomalies persist downstream to the order of 1 mmol m^{-3} in zonal average.

References

[1] Holzer, M., Primeau, F.W., DeVries, T., Matear, R.: The southern ocean silicon trap: Data-constrained estimates of regenerated silicic acid, trapping efficiencies, and global transport paths. Journal of Geophysical Research: Oceans **119**(1), 313–331 (2014) https://arxiv.org/abs/https://agupubs.onlinelibrary.wiley.com/doi/pdf/10.1002/2013JC009356. https://doi.org/10.1002/2013JC009356

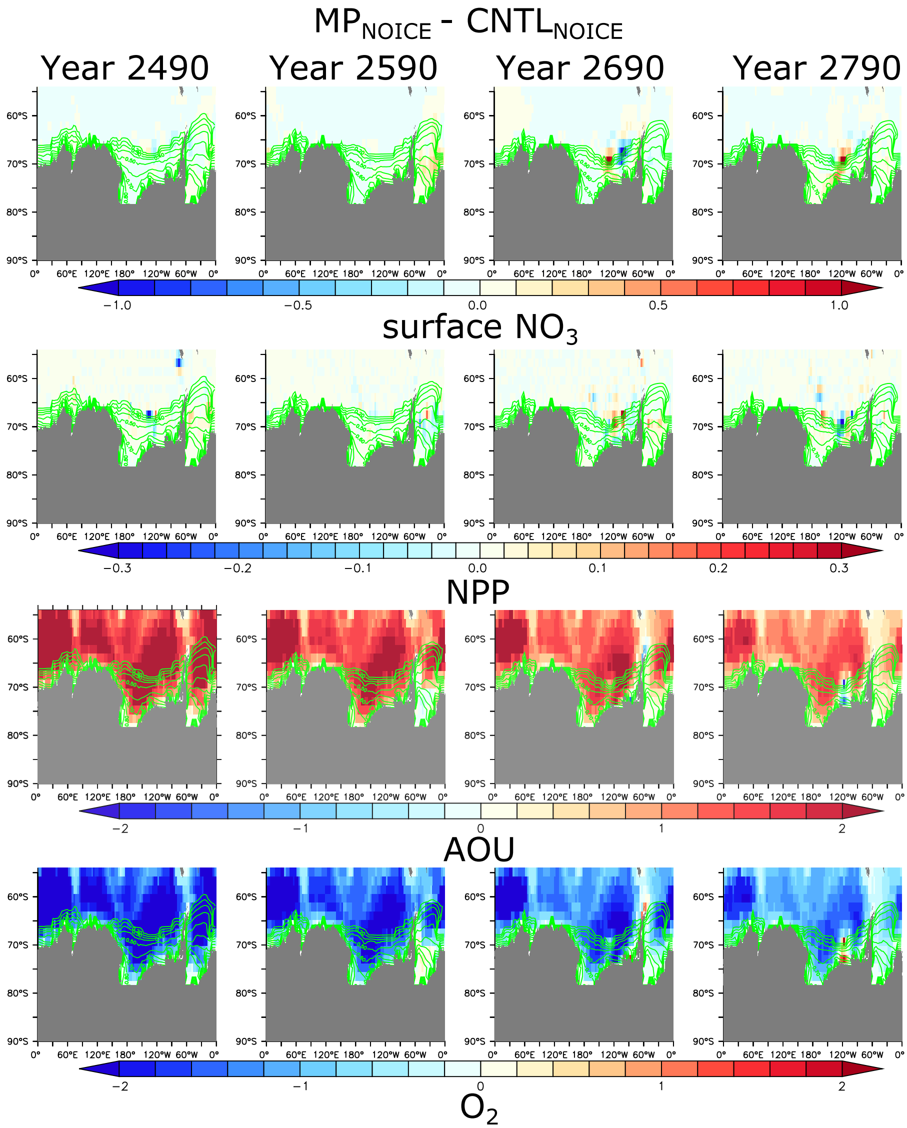

Fig. S3 MP_{NOICE}-$CNTL_{NOICE}$ anomalies of (top to bottom) surface nitrate in mmol m^{-3}, net primary production in mol N per year, water column average apparent oxygen utilisation (AOU=O_2sat-O_2 in mmol m^{-3}), and average water column oxygen in mmol m^{-3}. Green contours are annual average sea ice fraction.

[2] Taucher, J., Bach, L.T., Prowe, A.E.F., Boxhammer, T., Kvale, K., Riebesell, U.: Enhanced silica export in a future ocean triggers global diatom decline. Nature **605**(7911), 696–700 (2022). https://doi.org/10.1038/s41586-022-04687-0

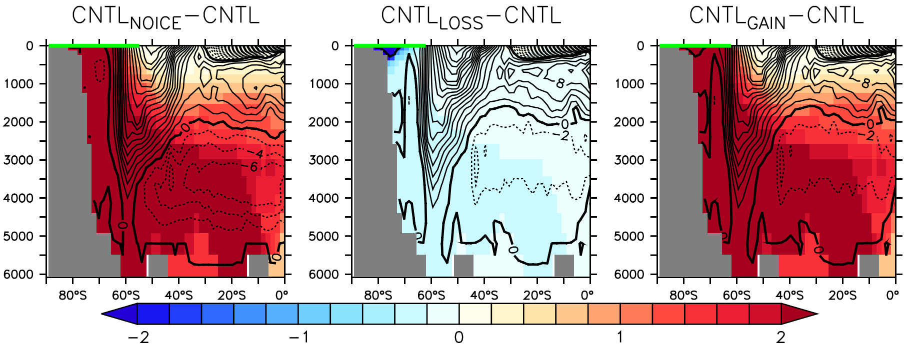

Fig. S4 Year 3000 zonally averaged oxygen anomalies in mmol m^{-3}. $CNTL_{NOICE}$-CNTL, left plot. $CNTL_{LOSS}$-CNTL, middle plot. $CNTL_{GAIN}$-CNTL, right plot.

[3] Krumhardt, K.M., Long, M.C., Lindsay, K., Levy, M.N.: Southern ocean calcification controls the global distribution of alkalinity. Global Biogeochemical Cycles **34**(12), 2020–006727 (2020) https://arxiv.org/abs/https://agupubs.onlinelibrary.wiley.com/doi/pdf/10.1029/2020GB006727. https://doi.org/10.1029/2020GB006727. e2020GB006727 10.1029/2020GB006727

[4] Koeve, W., Wagner, H., Kähler, P., Oschlies, A.: ^{14}c-age tracers in global ocean circulation models. Geoscientific Model Development **8**(7), 2079–2094 (2015). https://doi.org/10.5194/gmd-8-2079-2015

[5] Jambeck, J.R., Geyer, R., Wilcox, C., Siegler, T.R., Perryman, M., Andrady, A., Narayan, R., Law, K.L.: Plastic waste inputs from land into the ocean. Science **347**(6223), 768–771 (2015) https://arxiv.org/abs/https://science.sciencemag.org/content/347/6223/768.full.pdf. https://doi.org/10.1126/science.1260352

[6] Kvale, K., Prowe, A.E.F., Chien, C.-T., Landolfi, A., Oschlies, A.: The global biological microplastic particle sink. Scientific Reports **10**(1), 16670 (2020). https://doi.org/10.1038/s41598-020-72898-4